AN EVALUATION OF NUMERICAL MODELS FOR TEMPERATURE-STABILIZED COMBUSTION IN SMALL TUBES

G.M.G. Watson, G.P. Gauthier, and J.M. Bergthorson*
*jeff.bergthorson@mcgill.ca
Department of Mechanical Engineering, McGill University, 817 Sherbrooke West, Montréal, QC, Canada, H3A 2K6

Abstract

Flames stabilized in a heated tube with a diameter on the order of the flame thickness are investigated with numerical models of differing formulation. First, the two-dimensional structure of these flames is determined from a detailed model which solves the full, elliptic Navier-Stokes equations assuming axisymmetry. These solutions are then compared to those obtained from an often used, simpler 1-D volumetric model which relies on assumptions to model for wall/gas heat transfer. Volumetric models which use the standard assumption of constant Nusselt number have poor agreement with an average error of 18% (220 K) in wall temperature at the stabilization position. To correct this error the volumetric model is extended to employ a thermal boundary layer which uses a non-linear, radially-varying heat source to account for combustion and enhanced interfacial heat transfer inside the reaction zone. The extended model is very much improved with errors smaller than 2.5% (30 K) in wall temperature. This smaller deviation is caused by discrepancies in radial momentum and H species transport which are not accounted for in the volumetric model. Computational times range from minutes to several hours for the volumetric models, but are hundreds of hours for the detailed simulations.

Introduction

The study of flames in channels (in tubes or plates) is a fundamental problem which is relevant to new burner technologies [1]. These channels often have dimensions several times smaller than the quenching distance of the mixture. As a result, flames in these geometries are influenced by phenomena which can either quench or enhance flame propagation and stabilization. Flame dynamics are controlled by interfacial heat transfer to and from channel walls [2] and heat recirculation through them [3], radical quenching and surface reactivity [4], and other phenomena that depend on channel geometry and surface-to-volume ratio.

This study looks at the simplest case in this class of problem. It consists of a single tubular channel where the flame is decoupled from heat recirculation by a constant temperature wall. In such a system the combustion wave stabilizes at a single location in the monotonically increasing wall temperature profile. The restrictive nature of this case allows for fundamental study of the combustion wave and its proximity to the wall without the complications of a propagating thermal wave in the solid.

There is currently active research to determine the intricate interplay of kinetic and transport phenomena for these flames in a unified combustion model. Numerical modeling using computational fluid dynamics (CFD) is an important tool in this effort [5]. The proximity of the wall to the reaction zone generates multiple axial and transverse length scales. Therefore, multi-dimensional codes with multi-component physics, transport and detailed kinetic models are needed to accurately account for all phenomena in this problem. The most comprehensive codes are based on solving the complete Navier-Stokes equations, however these models are computationally expensive. As a result, most investigations with these equations resort to using simplified chemistry models [6, 7]. An alternative approach is to use a simpler formulation for the case approaching the limit where the reaction zone thickness is of the same order as the tube

radius:

$$\epsilon = \frac{\delta_{\mathrm{f}}}{r_{\mathrm{w}}} \rightarrow O(1), \tag{1}$$

where the flame thickness, which is the ratio of thermal diffusivity and laminar flame speed: $\delta_{\mathrm{f}} = \alpha / S_{\mathrm{L}}$, is $O(10^{-4})$ m for most hydrocarbon flames. For moderate inlet flow velocities, $S_{\mathrm{u}} < 5 S_{\mathrm{L}}$, flames are only weakly stretched with structures that are more or less flat and perpendicular to the oncoming reactant stream [8, 9]. In this formulation, it is assumed that the effect on burning rate due to inlet flow velocity, and the resulting flame curvature, is negligible in this limit and that simpler one-dimensional (1-D) volumetric equations are able to model the structure of these flames [10, 11].

Solutions from both models are obtained with a detailed, high temperature kinetics model for methane [12] which produce the first comprehensive CH_4/air solutions from detailed simulations. Flames are also simulated with a novel 1-D volumetric formulation which is extended to account for the effect of combustion on heat loss to the tube wall by coupling chemistry to a thermal boundary layer. Results from this model are validated against detailed simulations at different inlet flow velocities to test predictions of chemical structure and stabilization position. The results demonstrate that comparatively similar flame structures are attained from both models when the effects of non-linear heat release are accounted for in a consistent manner.

Numerical models

Consider a gas flowing into a domain restricted by a tubular duct with of inner wall radius, r_{w}, and a steady wall temperature profile, $T_{\mathrm{w}}(z)$. The coordinate system is 2-D and axisymmetric where the local gas temperature, t, velocity, u, and species mass fraction, y_k, vary radially, r, and axially, z. After a suitable hydrodynamic entrance length, the gas flows into the domain with an initial, uniform temperature profile, $t(r,0) = t_{\mathrm{u}}$, and fully developed parabolic velocity profile, $u(r,0) = 2S_{\mathrm{u}}\left(1 - \frac{r^2}{r_{\mathrm{w}}^2}\right)$, where S_{u} is the average inlet flow velocity.

Detailed flame model

A detailed model for this problem is based on the Navier-Stokes equations for low-Mach number reacting flows. The multi-dimensional, steady-state governing equations for mass, momentum, energy, and species, together with the equation of state for an ideal gas are below:

Continuity:

$$\nabla \cdot (\rho \vec{u}) = 0 \tag{2}$$

Momentum:

$$\rho \vec{u} \cdot \nabla \vec{u} = -\nabla p + \nabla \cdot (\mu \mathbf{S}) \tag{3}$$

Energy:

$$\rho \vec{u} \cdot \nabla h = \nabla \cdot (\rho \alpha \nabla h) \tag{4}$$

$$h = \sum_{k=1}^{N} Y_k h_k \qquad\qquad h_k = h_k^{\circ} + \int_{t_0}^{t} c_{p,k}\, \mathrm{d}t \tag{5}$$

Species:

$$\rho \vec{u} \cdot \nabla y_k = \nabla \cdot (\rho D_k \nabla y_k) + \dot{\omega}_k \tag{6}$$

State:

$$\rho = \frac{p \bar{W}}{RT}. \tag{7}$$

where $\mathbf{S}$ is the viscous stress tensor, D_k is the mixture averaged diffusion coefficient and $\dot{\omega}_k$ is the net production rate of species k. The energy equation is written in terms of total enthalpy,

therefore chemical reactions are included in the h term as it comprises the enthalpies of formation. The inter-species diffusion term is not included as its effect is assumed to be negligible.

For this problem axisymmetry is assumed, therefore a two-dimensional field for velocity, pressure, temperature and species is solved in the radial and axial directions. This is done utilizing a finite-volume discretization scheme in OPENFOAM. The momentum equation is appropriately formulated in order to use a SIMPLE (Semi-Implicit Method for Pressure Linked Equations) algorithm [13] that iteratively marches towards the steady-state solution. Detailed chemistry is handled using an operator-split method [14] which calculates a reaction rate based upon an Arrhenius kinetics integration over the residence time in each cell. These reaction rates, as well as thermodynamics and transport, are calculated using CANTERA. The reaction mechanism is chosen to be a reduced version of GRI-Mech 1.2 for high temperature chemistry that includes 19 species and 84 chemical reactions [12].

The above is a detailed model for this problem and thus accounts for all hydrodynamic, chemical and transport phenomena which produce the two-dimensional structure of these flames. This model is computationally expensive, however it is expected to give the most accurate representation of these flames for the assumed boundary conditions.

1-D volumetrically-averaged flame model

An alternative formulation is the 1-D volumetric model. The principle difference between this model and the detailed formulation is that radial variation is neglected and is replaced by volumetrically-averaged, bulk of parameters at each axial location. This formulation has been used by others to model this problem [10, 11], therefore the essential features are described here. The 1-D conservation equations are:

Continuity:

$$(\rho U)_z = \rho_\mathrm{u} S_\mathrm{u}, \tag{8}$$

Thermal energy:

$$\rho c_p U \frac{\mathrm{d}T}{\mathrm{d}z} = \frac{\mathrm{d}}{\mathrm{d}z}\left(\lambda \frac{\mathrm{d}T}{\mathrm{d}z}\right) - \sum_k c_{p,k} j_{k,z} \frac{\mathrm{d}T}{\mathrm{d}z} - \sum_k \dot{\omega}_k h_k W_k - Q_\mathrm{w}(z), \tag{9}$$

Species:

$$\rho U \frac{\mathrm{d}Y_k}{\mathrm{d}z} = -\frac{\mathrm{d}j_{k,z}}{\mathrm{d}z} + \dot{\omega}_k W_k, \tag{10}$$

where the upper-case variables are bulk parameters. Thermodynamic properties are defined by the bulk temperature and mass fractions and are linked through the equation of state (Equation 7). The variable $j_{k,z}$ is the diffusive mass flux of the species in the axial direction:

$$j_{k,z} = \rho Y_k V_{k,z}, \tag{11}$$

where $V_{k,z}$ is the mixture-averaged diffusion velocity in the axial direction [15] corrected by the bulk gas velocity. These equations are similar to those for conventional 1-D flames except for an additional term $Q_\mathrm{w}(z)$ in Equation 9 which accounts for the interfacial heat transfer between the wall and the gas. Similar algorithms can be used to solve the system of equations as long as an appropriate model for Q_w is specified.

Newton's law of cooling

The main difficulty in using the 1-D volumetric model is to account for the development of the thermal boundary layer which transfers energy to and from the wall. Since the bulk temperature

and composition are known, an expression is often cast based on Newton's law of cooling, which gives

$$Q_{\mathrm{w}}(z) = \frac{\lambda \mathrm{Nu}}{r_{\mathrm{w}}^2}(T - T_{\mathrm{w}}), \tag{12}$$

where Q_{w} is specified by a Nusselt number, Nu. An often-used approximation in reactive simulations is that interfacial heat transfer is similar to a thermally fully-developed non-reacting gas flow and that $\mathrm{Nu} \simeq 4.0$ [10, 11]. However, there is no clear reason to treat heat transfer within the reaction zone of a flame with this assumption as there may not be the time to reach a fully-developed profile due to the small axial thickness over which chemical enthalpy is converted to sensible enthalpy.

Boundary layer

An alternative model for interfacial heat transfer is needed which can account for the effect of chemical reactions on heat loss to the wall inside the reaction zone. This model reduces to two equations in axisymmetric coordinates which balance convection, radial diffusion and heat release by chemical reactions using standard boundary layer assumptions:

Thermal energy:

$$\rho c_p u \frac{\partial t}{\partial z} = \frac{\lambda}{r}\frac{\partial}{\partial r}\left(r\frac{\partial t}{dr}\right) - f(r,z)Q_{\mathrm{s}}(z), \tag{13}$$

Chemical enthalphy:

$$u\frac{\partial \zeta}{\partial z} = \frac{\lambda}{\rho c_p}\frac{\mathrm{Le}}{r}\frac{\partial}{\partial r}\left(r\frac{\partial \zeta}{\partial r}\right) - \dot{\zeta}, \tag{14}$$

Q_{s} is a source term which captures the effects of non-linear heat release by chemical reactions. Its magnitude is supplied by Equation 9 as the sum of conduction, interspecies diffusion and the heat of reaction terms in the flame to conserve axial energy. An additional assumption is that the radial velocity, v, is negligible compared to the axial flow. The velocity profile, u, is imposed as parabolic and is specified to satisfy continuity at the local axial gas density. Bypassing the momentum equation with this assumption means that the model does not have the capacity to account for radial mass flow due to the heat release from the flame.

Equation 14 describes the conservation of a progress variable for chemical enthalpy. The rate at which ζ is allowed to diffuse is controlled by a Lewis number, Le, which is defined here as the ratio of the diffusivity of ζ to thermal diffusivity. ζ is defined such that there is equivalence between its rate of consumption, $\dot{\zeta}$, and the rate at which energy is injected into the flow from the heat source:

$$\rho\dot{\zeta}(r,z) \equiv \frac{fQ_{\mathrm{s}}}{\left(\frac{\Delta E}{m}\right)_{\zeta}}. \tag{15}$$

ζ is unitless and behaves similar to the mass fraction of the deficient species, however it is a measure of chemical enthalpy. It is defined explicitly as the ratio of the heat of combustion of the composition at each location to that of the initial reactant mixture. Finally, $f(r,z)$ is a convolution which specifies the radial dependence of Q_{s}. It is assumed that the availability of the reactant species that ζ models limits the rate of chemical reactions, similar to the concentration of the deficient species in an Arrhenius term. The radial convolution, f, for the heat source term is, thus, made proportional to the local value of ζ:

$$f(r,z) = \frac{\zeta/Z}{2\int_0^{r_{\mathrm{w}}} \frac{r}{r_{\mathrm{w}}}\frac{\zeta}{Z}\,\mathrm{d}\left(\frac{r}{r_{\mathrm{w}}}\right)}, \tag{16}$$

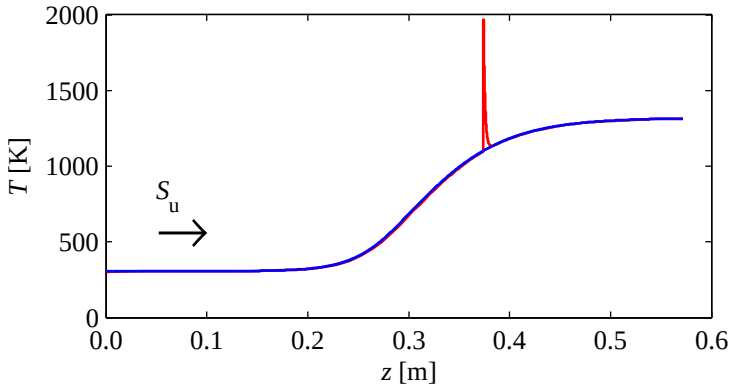

Figure 1: Computationally derived flame temperature structure from the volumetric model with the standard $\mathrm{Nu} = 4.0$ assumption. The gas temperature is in red while the wall temperature is in blue. $\phi = 1.0$, $S_\mathrm{u} = 0.85$ m/s.

where Z is the volumetrically averaged value of ζ at each axial location. The shape of ζ is retained in the definition of f, but the values are normalized to ensure conservation of the bulk heat release in the axial direction, or $\int f \, \mathrm{d}A/A = 1$.

The radial temperature profiles, $t(r, z)$, obtained in the solution to these equations are used to generate a profile for the interfacial heat transfer term, $Q_\mathrm{w}(z)$. The heat flux between the wall and the fluid is given by:

$$Q_\mathrm{w}(z) = -\frac{2\lambda}{r_\mathrm{w}} \frac{\partial t}{\partial r}\bigg|_\mathrm{w}, \tag{17}$$

which is proportional to the gas temperature gradient at the wall. This profile is continually updated in order to iteratively resolve the 1-D volumetric model.

Comparison of the models

In order to satisfy Equation 1, it is necessary to use a tube of small bore. A 1 mm internal diameter tube is used as a compromise between this condition and the quenching distance for the achievable wall temperature found in experiments for this case [2, 10]. In these experiments, radiant heaters impose a smooth temperature profile along the wall of the tube which is uniform along the tube perimeter, but increases monotonically with downstream distance. As the gas enters this region, it is heated by interfacial heat transfer from the wall. Under these conditions a stable, symmetric flame will stabilize in the tube downstream from the entrance. As the mixture approaches it, the chemistry becomes activated to feed the flame when the rate at which sensible energy gained from heat release and heat transfer overcomes the rate at which energy is lost to the wall.

Figure 1 shows a typical wall temperature profile and bulk gas temperatures obtained from the computation. The wall temperature increases monotonically between 300 K and 1320 K. Three characteristic zones can be identified in the gas temperature profile. In the first zone, the gas temperature is lower than the wall temperature. Heat is convectively transferred from the hot wall to the gas raising its temperature and enthalpy. In the second zone, the activation of the reactions causes a rapid rise in temperature due to a concentration of enthalpy in this zone. The position of this zone depend on a balance of the energy released from chemical reactions and heat loss to the wall. After the gas reaches its maximum temperature, its temperature drops abruptly in the third zone due to intense interfacial heat exchange with the cooler wall. The wall temperature is lower than the adiabatic flame temperature in this region.

A summary of flame position data obtained from the simulations versus inlet velocity is shown

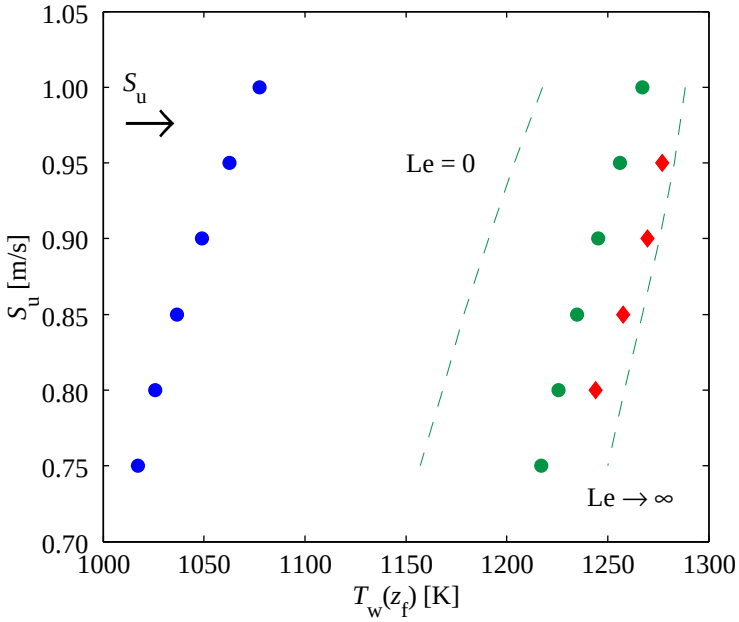

Figure 2: Inlet flow velocity, S_{u}, verses simulated wall temperature at the flame stabilization position, $T(z_{\mathrm{f}})$, in a $D = 1$ mm tube. Models are the 1-D volumetric model which uses $\mathrm{Nu} = 4.0$ (blue circles) and a boundary layer solution which incorporates heat release, $\mathrm{Le} = 1.0$ (green circles), and the detailed model (red diamonds).

in Figure 2. The stoichiometric flames used in this study are established in the range $0.75\ \mathrm{m/s} \leq \mathrm{S_u} \leq 1.00\ \mathrm{m/s}$, and are strongly burning, stable, symmetric flames that have a unique stabilization position within the wall temperature profile. In Figure 2, the flame position moves downstream to higher wall temperatures with increasing inlet flow velocity. Energy needed to heat the large flux of reactants must be balanced by heat gain from wall heat transfer and chemical reactions. When the flame is perturbed by higher flow velocities it requires more energy to heat the reactants due to the increased mass flow entering the system. Reaction rate is a function of temperature, therefore the flame cannot immediately adjust to the added mass flow by generating higher heat release due to chemical reactions. It must therefore move to a higher temperature location in the tube where the energy needed can be balanced by increased heat transfer from the tube wall and higher reaction rates at the increased local temperature.

Flames simulated with the volumetric model and the standard Nusselt number assumption predict positions which are consistently far upstream from those predicted by the detailed formulation. There is considerable disagreement with predicted flame positions being an average of 145 flame thicknesses upstream, or an average deviation of 220 K in wall temperature[1]. These positions are also upstream from the $\mathrm{Le} = 0.0$ limit, which represents the lowest possible heat loss for a flame when 2-D effects of chemical energy release on the thermal boundary layer are considered. The upstream deviations in flame position are a direct result of the under-prediction of heat loss inside the reaction zone. In contrast to the volumetric solution with the standard Nusselt number assumption, inclusion of the heat source term and boundary layer in the extended volumetric formulation, with $\mathrm{Le} = 1.0$, predicts flames which are on average 33 flame thicknesses upstream from the detailed simulations. These deviations are no greater than 30 K in wall temperature throughout the velocity range. The agreement between the detailed and ex-

[1]Flame thickness is calculated from the simulated flame profiles using twice the full-width at half maximum of the Q_{s} profile. This width contains 98% of the integrated fitted gaussian profile.

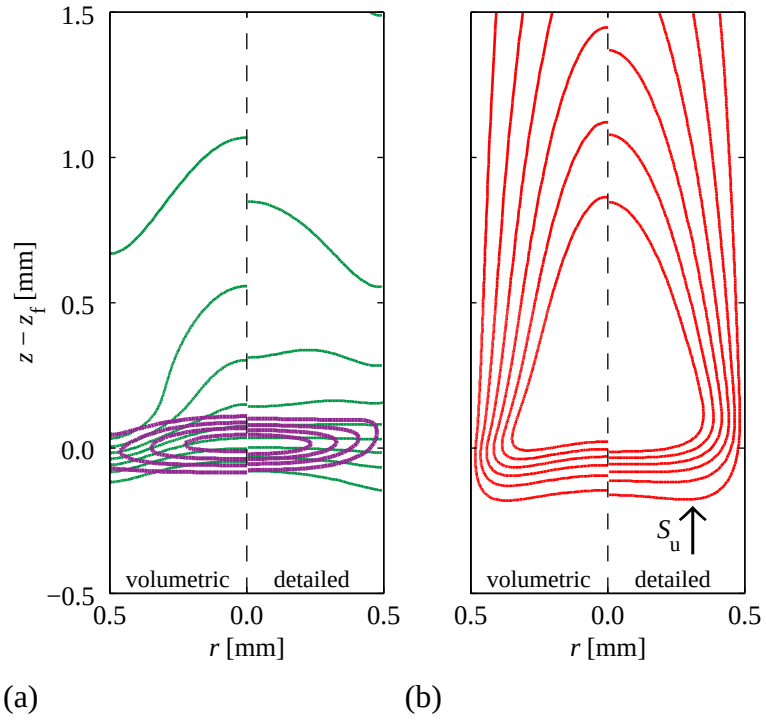

(a) (b)

Figure 3: Contour profiles from the 1-D volumetric flame model (left) and detailed flame model (right) in a $D = 1$ mm tube: $\phi = 1.0$, $S_{\mathrm{u}} = 0.85$ m/s. The contours show (a) Q_{s} (thick line) and ζ (thin line), and (b) Gas temperature profiles, $t - T_{\mathrm{w}}$.

tended volumetric models is very much improved, but the volumetric model does consistently predict stronger flames.

Figure 3 shows a comparison of the axisymmetric structure of the flame for the extended volumetric and detailed models. The 1-D volumetric flame model is shown as a series of ζ and Q_{s} contours that account for chemistry in the boundary layer and the resulting temperature contours, $t - T_{\mathrm{w}}$. The contours of ζ and Q_{s} in Figure 3(a) indicate that most of the chemical activity in the flame is in a small region centered around the reaction zone. This area governs flame behavior and position. Figure 3(b) shows the gas temperature in the vicinity of this region. As heat is released chemical enthalpy is initially consumed at higher rates near the walls because ζ is advected into the reaction zone at a higher rate near the centerline due to the velocity profile and the no-slip condition at the wall. A rise in the gas temperature is coincident with the consumption of reactants and accompanying heat release. When the source term dissipates, the gas temperature continues to rise near the centerline due to slower ζ consumption in the CO oxidation region of the flame while the gas temperature rapidly cools at the walls due to intense interfacial heat exchange.

It is useful to consider how the volumetric contours would change at the upper and lower limits of the Lewis number. When $\mathrm{Le} = 0$, chemical enthalpy does not diffuse in the radial direction, thus ζ consumed at the walls would not be replenished by diffusion. Heat release would concentrate at the centerline where the flux of chemical enthalpy is the highest, producing shallower temperature gradients at the wall. Conversely when $\mathrm{Le} \to \infty$, chemical enthalpy is much more diffusive than heat. Its consumption at the wall would rapidly be replenished by ζ from the centerline. The resulting ζ profile would be radially uniform owing to high diffusivity that would smooth out any gradients producing uniform heat release across the channel. The $\mathrm{Le} \to \infty$ solution has the maximum amount of energy released near the wall resulting in the

steepest gradients and the highest possible heat loss for this extended volumetric model.

The temperature contours of the models in Figure 3(b) are in reasonable agreement in terms of value and spatial extent. However, radial boundary layer profiles for chemical enthalpy show noticeable deviation from the detailed model. This is especially apparent inside of the reaction zone of the detailed model where the ζ contours are locally radially uniform, similar to the what would be results from a $\mathrm{Le} \to \infty$ boundary layer model.

Discrepancies

The extended volumetric model offers improved predictions for flame position which are closer to the detailed simulations, however deviation from the true value remains. This deviation is caused by small discrepancies in species and momentum which can be seen by comparing the volumetric and detailed profiles.

Species profiles

Spatial profiles of species and their chemical rates have an important impact on these models. It is essential to ensure that these are accurately predicted in the volumetric model to ensure the correct burning rate. Figure 4 shows contour plots for a selection of permanent (CH_4, O_2, H_2O and CO_2) and intermediate species (CO, CH_3) mole fractions from the detailed model for an intermediate inlet flow velocity. These profiles have a definite 2-D structure which is produced by the non-uniform flow profile and radial diffusivity. Reactants CH_4 and O_2 which convect into the flame are initially consumed at the walls. Consumption of these species correspond to production of CH_3 and CO in the primary reaction zone, around $z - z_\mathrm{f} = 0$, and the subsequent production of H_2O and CO_2 in the post-flame region.

Volumetric models yield solutions that must be considered as spatially-averaged in the radial direction. Therefore, bulk composition is used to compare these solutions to those obtained by the detailed model. Figure 5 show axial profiles for permanent species mole fractions from both models. There is excellent agreement for all species profiles which suggests that the volumetric model does a good job predicting overall conversion rates for this case. Figure 6 shows a selection of intermediate species profiles in the immediate vicinity of the flame. These profiles also show good agreement in shape, however the volumetric model significantly underpredicts concentrations of the heavier C_2 species upstream from the flame. This deviation is largely a temperature effect due to low temperature chemistry and is caused by the difference in flame position within the wall temperature profile predicted by both models.

The concentration of the free radicals O, OH and H play an important role in decomposition of methane through H abstraction and regulate burning rate. Averaged axial profiles of these species are shown in Figure 7 while radial contours from the detailed profile are shown in Figure 8. There is good agreement in the bulk concentration of O and OH radicals, however the volumetric model significantly over-predicts the concentration of H throughout the flame. This behavior coincides with differences in the radial extent of species contours. In Figure 8, regions with increased O and OH mole fraction closely match regions with the highest temperatures. However in contrast to all other intermediate species, H is more uniform across the channel due to its much higher diffusivity. Over prediction of the concentration of H would produce higher burning rates which could be one reason why the volumetric model consistently predicts stronger flames.

Flow redirection

Flow acceleration is produced inside a flame due to rapid temperature rise and the resultant drop in density. In a small tube, this dilatation is essentially a source of momentum which pushes on the flow in all directions and can cause non-negligible radial velocity components. This

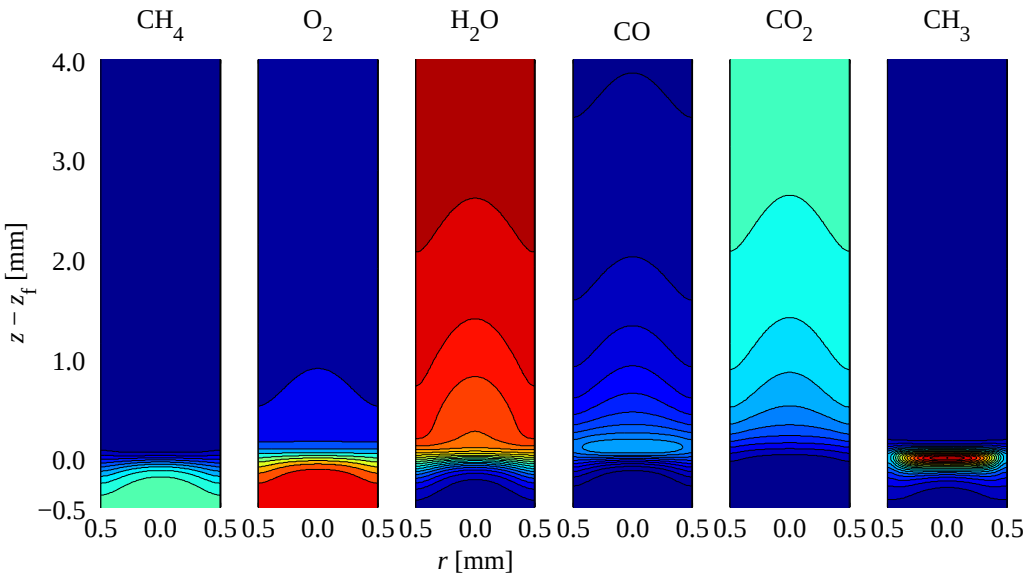

Figure 4: 2-D, axisymmetric contours of the permanent and intermediate predicted by the detailed model. $\phi = 1.0$, $S_{\mathrm{u}} = 0.85$ m/s.

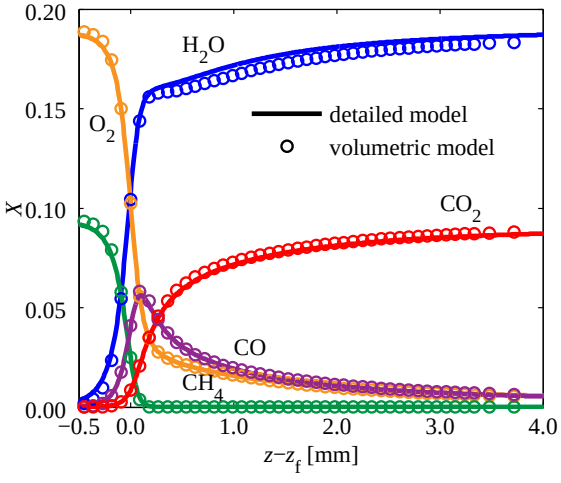

Figure 5: Comparison of axial profiles of permanent species mole fractions. Operating conditions as in Figure 4.

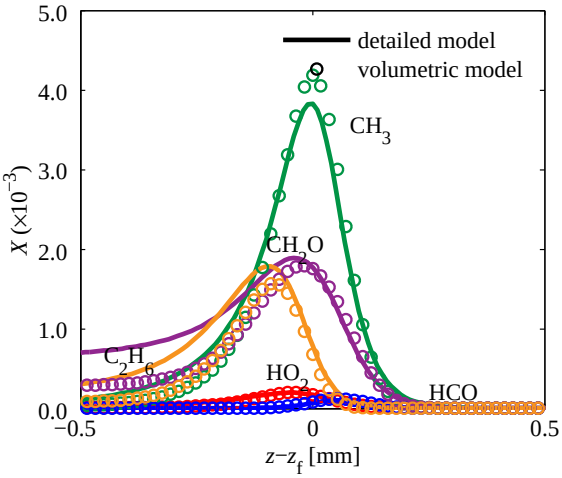

Figure 6: Comparison of axial profiles of some intermediate species mole fractions. Operating conditions as in Figure 4.

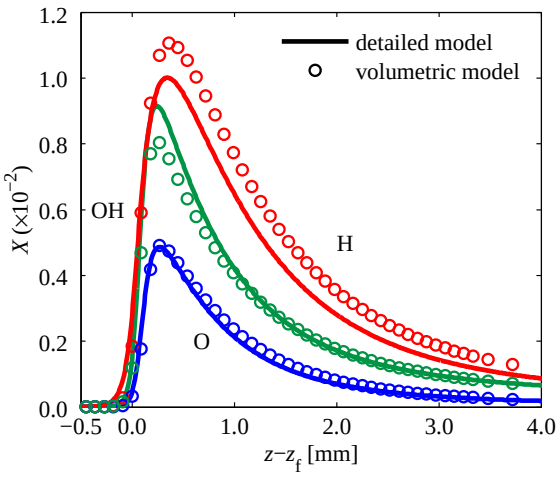

Figure 7: Comparison of axial profiles of free radical mole fractions O, OH and H. Operating conditions as in Figure 4.

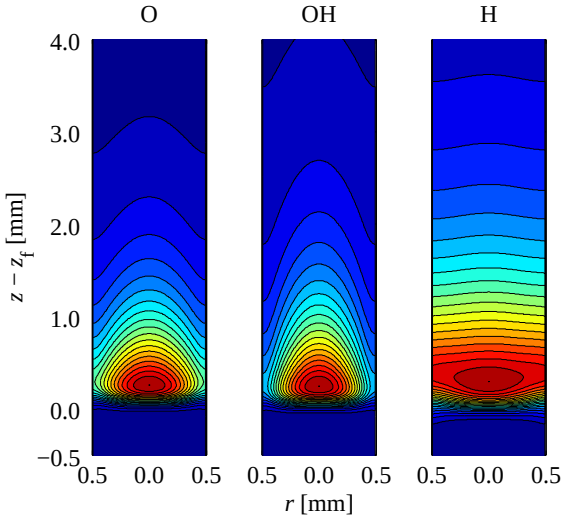

Figure 8: 2-D, axisymmetric contours of free radicals from the detailed model. Operating conditions as in Figure 4.

phenomenon has been called flow redirection by others [9] and is found to significantly affect burning rate in meso-scale tubes. In this section, the volumetric assumption of a parabolic axial profile and an insignificant radial component in the limit of small ϵ is evaluated by comparison with solutions from the detailed simulation.

Figure 9 shows deviations in axial and radial mass flux ($\Delta\rho u$ and $\Delta\rho v$) from the assumed axial parabolic profile at axial locations $z - z_{\rm f}$ in the vicinity of the flame. The definitions for these deviations are

$$\begin{aligned} \Delta\rho u &= \frac{\rho(t)u - 2\rho(T)U\,(1-(r/r_{\rm w})^2)}{\rho_{\rm u}S_{\rm u}}, \\ \Delta\rho v &= \frac{\rho(t)v - 0}{\rho_{\rm u}S_{\rm u}}, \end{aligned} \tag{18}$$

where they are normalized by the average axial mass flow ($\rho_{\rm u}S_{\rm u}$), which is a conserved quantity in both models. Density in these relations are specified either at the local temperature, $t(z,r)$, or as an average at the bulk temperature, $T(z)$, and composition.

The flow profile does deviate from parabolic in a small zone in the vicinity of the flame (-0.5 mm$< z - z_{\rm f} <$ 2.0 mm). When this occurs axial mass flow drops at the centreline and is higher at the wall due to transition to a top-hat profile. However, a top-hat profile is not achieved before the flow begins to develop back to the parabolic profile. The axial variation of mass flow is strong enough to produce a radial outflow which is approximately 1/10th of the average mass flux at the flame location. Radial convection of reactants towards the wall broadens heat release in a similar way to the enhanced diffusion of the $\mathrm{Le} \to \infty$ case.

Conclusion

Alternative formulations for combustion stabilized by a wall temperature profile in a 1 mm tube have been compared for the full range of inlet flow velocities which produce strongly burning flames. The detailed formulation has few assumptions and is expected to be valid for the assumed boundary conditions, but is computationally costly to implement. The simple, volumetric formulation has much lower computational cost, but lower accuracy. However, this can

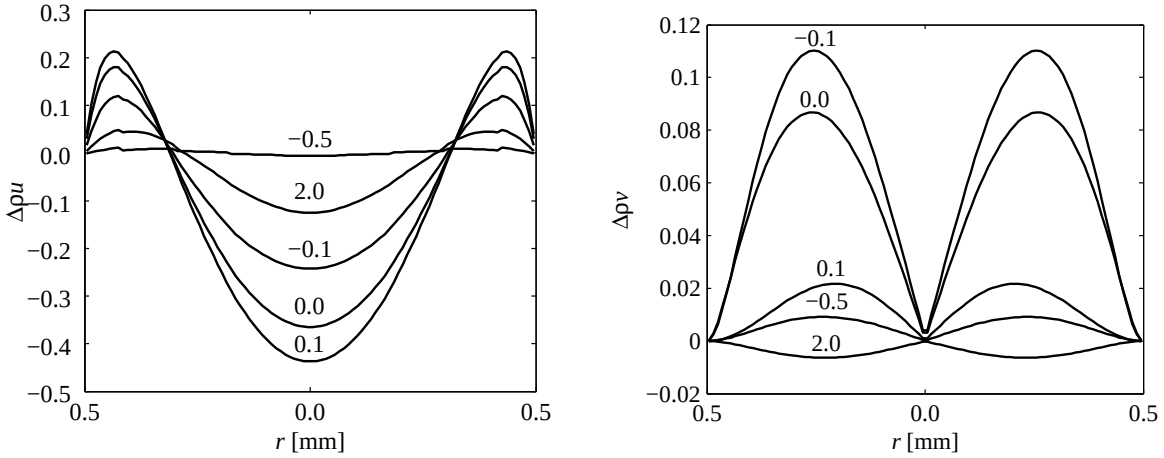

(a) (b)

Figure 9: Deviations in axial (a) and radial (b) mass flow from an assumed parabolic profile. Profiles are extracted from the detailed model at axial locations $z - z_{\mathrm{f}}$ =-0.5, -0.1, 0.0, 0.1, 2.0 mm. $\phi = 1.0$, $S_{\mathrm{u}} = 0.85$ m/s.

be significantly improved by incorporating a boundary layer model for interfacial heat transfer into the formulation.

The spatial details of heat release are also found to be important for these strongly burning flames. In the volumetric formulation, the boundary layer calculation replaces common assumptions for Nusselt number with a model built around the conservation of chemical enthalpy and the effects of its conversion to sensible enthalpy in the flame. The model gives improved results, but the use of a fixed parabolic velocity profile and bulk properties and composition are approximations that limit accuracy. The volumetric model also has application only to tubes of small diameters (small ϵ) which exhibit "flat" flames. However, the accuracy of this model is very much improved when comparisons are made with detailed simulations. This result demonstrates that heat loss by interfacial heat transfer is the dominant phenomenon that defines the position of these flames.

Acknowledgements

Computing resources for this study were provided by the "Consortium Laval, Universite du Quebec, McGill and Eastern Quebec" (CLUMEQ). Finally, funding from the Natural Sciences and Engineering Research Council of Canada and the "Fonds Quebecois de la Recherche sur la Nature et les Technologies" is acknowledged.

References

[1] K Maruta. Micro and mesoscale combustion. *Proc. Combust. Inst.*, 33, 2010. in press.

[2] GA Fateev, OS Rabinovich, and MA Silenkov. Oscillatory combustion of a gas mixture blown through a porous medium or a narrow tube. *Proc. Combust. Inst.*, 27:3147–53, 1998.

[3] T Takeno and K Sato. An excess enthalpy flame theory. *Combust. Sci. Tech.*, 20:73–84, 1979.

[4] KT Kim, DH Lee, and S Kwon. Effects of thermal and chemical surface-flame interaction on flame quenching. *Combust. Flame*, 146:19–28, 2006.

[5] G Pizza, CE Frouzakis, J Mantzaras, AG Tomboulides, and K Boulouchos. Dynamics of premixed hydrogen/air flames in microchannels. *Combust. Flame*, 152:433–50, 2008.

[6] CL Hackert, JL Ellzey, and OA Ezekoye. Combustion and heat transfer in model two-dimensional porous burners. *Combust. Flame*, 116:177–91, 1999.

[7] DG Norton and DG Vlachos. A CFD study of propane/air microflame stability. *Combust. Flame*, 138:97–107, 2004.

[8] J Daou and M Matalon. Flame propagation in poiseuille flow under adiabatic conditions. *Combust. Flame*, 124:337–49, 2001.

[9] NI Kim and K Maruta. A numerical study on propogation of premixed flames in small tubes. *Combust. Flame*, 146:283–301, 2006.

[10] K Maruta, T Kataoka, NI Kima, S Minaev, and R Fursenko. Characteristics of combustion in a narrow channel with a temperature gradient. *Proc. Combust. Inst.*, 30:2429–36, 2005.

[11] Y Ju and B Xu. Theoretical and experimental studies on mesoscale flame propagation and extinction. *Proc. Combust. Inst.*, 30:2445–53, 2005.

[12] H Wang and M Frenklach. Detailed reduction of reaction mechanism for flame modeling. *Combust. Flame*, 87:365–70, 1991.

[13] SV Pantakar. *Numerical heat transfer and fluid flow, First Edition*. McGraw-Hill, New York, 1980.

[14] NN Yanenko. *The Method of Fractional Steps*. Springer, New York, 1971.

[15] RJ Kee, ME Coltrin, and P Glarborg. *Chemically Reacting Flow: Theory and Practice*. John Wiley, New York, 2003.